

000 001 002 003 004 005 006 007 008 009 010 011 012 013 014 015 016 017 018 019 020 021 022 023 024 025 026 027 028 029 030 031 032 033 034 035 036 037 038 039 040 041 042 043 044 045 046 047 048 049 050 051 052 053 CoLA: A CHOICE LEAKAGE ATTACK FRAMEWORK TO EXPOSE PRIVACY RISKS IN SUBSET TRAINING

Anonymous authors

Paper under double-blind review

ABSTRACT

Subset training, where models are trained on a carefully chosen portion of data rather than the entire dataset, has become a standard tool for scaling modern machine learning. From coresnet selection in vision to large-scale filtering in language models, these methods promise scalability without compromising utility. A common intuition is that training on fewer samples should also reduce privacy risks. In this paper, we challenge this assumption. We show that subset training is not privacy free: the very choices of which data are included or excluded can introduce new privacy surface and leak more sensitive information. Such information can be captured by adversaries either through side-channel metadata from the subset selection process or via the outputs of the target model. To systematically study this phenomenon, we propose CoLa (Choice Leakage Attack), a unified framework for analyzing privacy leakage in subset selection. In CoLa, depending on the adversary’s knowledge of the side-channel information, we define two practical attack scenarios: Subset-aware Side-channel Attacks and Black-box Attacks. Under both scenarios, we investigate two privacy surfaces unique to subset training: (1) Training-membership MIA (TM-MIA), which concerns only the privacy of training data membership, and (2) Selection-participation MIA (SP-MIA), which concerns the privacy of all samples that participated in the subset selection process. Notably, SP-MIA enlarges the notion of membership from model training to the entire data–model supply chain. Experiments on vision and language models show that existing threat models underestimate the privacy risks of subset training: the enlarged privacy surface not only retains training membership leakage but also exposing selection membership, extending risks from individual models to the broader ML ecosystem.

1 INTRODUCTION

The scale of modern datasets has made training on the full corpus increasingly impractical. To address this, practitioners routinely employ subset training, where only a carefully chosen ratio of data is used. This paradigm is adopted not only for efficiency but also to improve data quality, since selection can remove redundancy and noise while retaining informative samples. Subset training spans diverse applications: coresnet selection (Bachem et al., 2015; Munteanu et al., 2018; Mirzasoleiman et al., 2020) in vision, dataset pruning (Sorscher et al., 2022; Yang et al., 2022; Qin et al., 2023), active learning (Sener & Savarese, 2018; Ducoffe & Precioso, 2018; Agarwal et al., 2020) in general ML, and large-scale deduplication (Lee et al., 2022), filtering (Rae et al., 2021), and sampling (Guneskar et al., 2023; Peng et al., 2025; Wettig et al., 2024) in language model pretraining.

While subset training is widely celebrated for these benefits, its privacy implications remain under-explored (Zhao & Zhang, 2025). A common intuition suggests that fewer training samples should imply less privacy leakage (Dong et al., 2022). Yet this reasoning overlooks an important fact: *the choices made during subset selection themselves encode signals about which data were included and which were excluded*. These signals can be inherited through shifts in the data distribution or model behavior, making them exploitable by adversaries.

We ask the fundamental question: *Does subset training actually reduce privacy leakage?* Our answer is *no*. We show that subset training introduces new attack surfaces: not only is the included data that used for training compromised, but the excluded data discarded from training can also become

vulnerable due to correlations introduced by the selection mechanism. In other words, due to the data-oriented nature of the subset selection process, beyond the training data leakage emphasized by traditional MIA (Shokri et al., 2017; Hu et al., 2022), the choice signals further extend privacy risks from individual models to the broader data–model supply chain. Accordingly, we define two complementary privacy surfaces: *Training-membership MIA (TM-MIA)*, which resembles traditional MIA by focusing on the membership of training data, and *Selection-participation MIA (SP-MIA)*, a privacy surface tailored to subset training that focuses on membership at the data selection level.

To systematically study membership leakage under these privacy surfaces, we propose **CoLa (Choice Leakage Attack)**, a framework that leverages choice signals in a principled way to conduct attacks across different surfaces. CoLa captures risks under two complementary settings: (i) a *Subset-aware Side-channel* setting, where the adversary has access to the target model’s outputs and selection metadata (e.g., the selection algorithm and the inclusion ratio); and (ii) a *Black-box* setting, where the adversary observes only model outputs and is aware that subsetting may have been used, without knowing any selection metadata. Extensive results show that for both privacy surfaces under these two attack settings, CoLa can substantially strengthen the attack performance. In short, subset training does not guarantee privacy; it enlarges the attack surface of modern ML pipelines and highlights the need to protect privacy across the entire data–model supply chain. We summarize our contributions as follows:

- We provide the first systematic definition and exploration of the membership leakage problem under subset training. This novel attack scenario reveals a severe privacy risk in the subset selection process: not only is the privacy of training data compromised, but the data excluded during selection is also at risk.
- We propose CoLa (Choice Leakage Attack), a framework tailored to subset selection that leverages choice signals in a principled way for more reliable membership inference, while seamlessly unifying diverse attack settings and surfaces.
- Experiments across both vision and language models confirm the broad capability of CoLa. For example, in the black-box setting, the AUC of CoLa on Pythia-160M surpasses 80% under SP-MIA, where all baseline methods fail.

2 RELATED WORKS

Subset training and data-efficient learning. A large body of research has explored how to reduce the cost of large-scale training by operating on subsets of data. Coreset selection constructs small but representative subsets that approximate training on the full data (Bachem et al., 2015; Munteanu et al., 2018; Mirzaoleiman et al., 2020; Yang et al., 2024b). Dataset pruning removes redundant or low-value samples to improve efficiency and generalization (Sorscher et al., 2022; Yang et al., 2022; Qin et al., 2023; Maharana et al., 2023; Tan et al., 2024). Active learning queries the most informative examples to reduce annotation cost (Sener & Savarese, 2018; Ducoffe & Precioso, 2018; Agarwal et al., 2020; Borsos et al., 2020; Margatina et al., 2021). In large-scale language models, deduplication and filtering pipelines are routinely applied to eliminate noise and improve training quality (Lee et al., 2022; Rae et al., 2021; Raffel et al., 2023; Gao et al., 2020a). These techniques have been extensively studied for efficiency and utility, but their privacy consequences remain largely underexplored.

Membership inference attacks. Membership inference attacks (MIAs) are among the most widely studied privacy threats in machine learning. Early work by Shokri et al. (2017) proposed shadow models to train attack classifiers distinguishing members from nonmembers. Subsequent methods exploited confidence scores, loss values, or gradients (Yeom et al., 2018; Sablayrolles et al., 2019; Carlini et al., 2022b). MIAs have been demonstrated in supervised learning, federated learning, and large language models (Nasr et al., 2018; Hu et al., 2022; Li et al., 2025), motivating defenses such as differential privacy (Abadi et al., 2016) and adversarial regularization (Nasr et al., 2018). This body of work reveals how models trained on fixed datasets can memorize and leak sensitive information. However, they primarily focus on constructing membership signals in a one-shot manner, with these signals being tightly coupled to a specific model. We find such model-oriented signal less effective in the context of subset training. Leveraging the unique characteristics of the subset selection process, we instead construct membership signals in a data-oriented manner.

108 **Synthetic data and privacy.** Synthetic data generation has been studied as a way to train models
 109 without exposing raw datasets, with the promise of stronger privacy (Hu et al., 2024; Tan et al.,
 110 2025). However, subsequent research has shown that synthetic datasets can still leak sensitive in-
 111 formation about the original data, including membership and attributes (Stadler et al., 2022; van
 112 Breugel et al., 2023; Zhao & Zhang, 2025). Rather than analyzing risks inherent in *synthetic data*
 113 *generation pipelines*, we turn to *subset training with real data*, where high-fidelity samples remain
 114 but the selection process itself exposes a distinct and overlooked channel of privacy leakage.

116 3 PROBLEM SETTING

118 3.1 MEMBERSHIP INFERENCE UNDER SUBSET TRAINING

120 Let $D_0 \subseteq \mathcal{X} \times \mathcal{Y}$ denote the original dataset that undergoes a subset selection procedure. A selector
 121 $\text{Sel}(\cdot; r)$ with a given selection ratio r partitions D_0 into two disjoint sets: the **included data** I used
 122 for training, and the **excluded data** E that are discarded:

$$123 (I, E) = \text{Sel}(D_0; r), \text{ with } I \cap E = \emptyset, I \cup E = D_0, |I|/|D_0| = r. \quad (1)$$

125 Following the standard MIA pipeline (Shokri et al., 2017), we further denote by O the **outside data**
 126 that never enter the selection process. A model f_θ is trained solely on I . This partition naturally
 127 induces two types of membership inference task:

128 **Training-membership MIA (TM-MIA).** This attack takes the model itself as the attack surface and
 129 membership is defined solely by the training data. A sample x is a member if $x \in I$ and nonmember
 130 if $x \in E \cup O$. This forms a natural and widely
 131 adopted threat model, as the model is the most
 132 direct output of the ML system. This setting is
 133 consistent with conventional MIAs (Shokri et al.,
 134 2017; Carlini et al., 2022b).

135 **Selection-participation MIA (SP-MIA).** However, when the attack surface is enlarged to the
 136 entire data–model pipeline, membership expands
 137 from only the training data to a much larger por-
 138 tion of all collected data. As shown in Figure 1, we refer to the collected data as selection members,
 139 where a sample x is a member if $x \in I \cup E$ and a non-member if $x \in O$. Its membership cannot
 140 be explained by direct model memorization, but instead reveals *choice leakage*, a side-channel sig-
 141 nal from the subset selection process of the data–model supply chain. Such choice leakage risk is
 142 severe as it exposes a system’s selection preferences. Once the data–model supply chain is exposed
 143 to privacy risks, the entire pipeline, from raw data to model outputs, becomes vulnerable to mal-
 144 cious manipulation. **To our knowledge, this is the first work to systematically investigate this**
 145 **perspective.**

146 Both tasks can be framed as binary hypothesis tests over a scoring function $s : \mathcal{D}_0 \rightarrow \mathbb{R}$, which
 147 measures the likelihood of a sample x belonging to the respective member set. Given $\mathcal{D}_0 = I \cup E \cup O$,
 148 the member–nonmember partitions are:

$$149 \mathcal{M}_{\text{TM}} = I, \quad \mathcal{N}_{\text{TM}} = E \cup O, \quad (2)$$

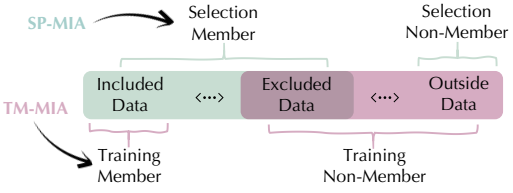
$$150 \mathcal{M}_{\text{SP}} = I \cup E, \quad \mathcal{N}_{\text{SP}} = O. \quad (3)$$

152 The goal is to design a scoring function $s(x)$ that distinguishes \mathcal{M} from \mathcal{N} under both definitions.

154 3.2 ADVERSARY KNOWLEDGE

156 Subset training changes not only the definition of membership but also the adversary’s potential
 157 knowledge and capabilities. We consider two complementary scenarios:

158 **Subset-aware side-channel attacks.** In line with the common assumption in prior MIAs, the adver-
 159 sary can query the deployed model f_θ and observe its outputs (e.g., prediction labels or confidence
 160 scores). In addition, it has access to *side information about the selection process*, such as the strategy
 161 used (e.g., coresset selection, pruning, filtering) or the approximate inclusion ratio. Such an assump-
 162 tion is realistic: pruning papers routinely report retained percentages to justify efficiency–utility



153 Figure 1: Privacy surfaces under subset training.

154

155

156

157

158

159

160

161

162

163

164

165

166

167

168

169

170

171

172

173

174

175

176

177

178

179

180

181

182

183

184

185

186

187

188

189

190

191

192

193

194

195

196

197

198

199

200

201

202

203

204

205

206

207

208

209

210

211

212

213

214

215

216

217

218

219

220

221

222

223

224

225

226

227

228

229

230

231

232

233

234

235

236

237

238

239

240

241

242

243

244

245

246

247

248

249

250

251

252

253

254

255

256

257

258

259

260

261

262

263

264

265

266

267

268

269

270

271

272

273

274

275

276

277

278

279

280

281

282

283

284

285

286

287

288

289

290

291

292

293

294

295

296

297

298

299

300

301

302

303

304

305

306

307

308

309

310

311

312

313

314

315

316

317

318

319

320

321

322

323

324

325

326

327

328

329

330

331

332

333

334

335

336

337

338

339

340

341

342

343

344

345

346

347

348

349

350

351

352

353

354

355

356

357

358

359

360

361

362

363

364

365

366

367

368

369

370

371

372

373

374

375

376

377

378

379

380

381

382

383

384

385

386

387

388

389

390

391

392

393

394

395

396

397

398

399

400</

162 trade-offs, active learning and coresets methods describe selection strategies for reproducibility, and
 163 large-scale LLM pipelines release dataset cards documenting filtering heuristics, inclusion ratios, or
 164 deduplication statistics (Cohen-Addad et al., 2021; Biderman et al., 2023a; Dubey et al., 2024; Yang
 165 et al., 2024a). Crucially, this information reflects only high-level rules, not the exact membership
 166 of individual samples. Our attack targets precisely this gap: even when only the selection algorithm
 167 or ratio is public, an adversary can exploit this side-channel to infer which specific samples were
 168 included or excluded, thereby exposing *choice leakage* in subset training.

169 **Black-box attacks.** Here the adversary can only query the deployed model f_θ and observe its out-
 170 puts. The entire subset selection stage is hidden, so the adversary must rely solely on the observable
 171 behavior of the trained model or the intrinsic data-specific information. This setting captures the
 172 most restrictive and widely assumed threat model in prior MIA research (Hu et al., 2022).

174 4 METHOD

175 4.1 CHALLENGES OF MEMBERSHIP INFERENCE UNDER SUBSET TRAINING

178 In conventional MIA, success comes from exploiting overfitting: models tend to assign systemati-
 179 cally higher confidence to their training data than to non-members. Under subset training, however,
 180 this signal becomes entangled. Figure 2 illustrates this using the LiRA attack signal from (Carlini
 181 et al., 2022b) on a model trained on I selected from D_0 by Glister (Killamsetty et al., 2021b). The
 182 dataset used here is CIFAR10 and the model is ResNet18. Since the selector is designed to make
 183 training on I approximate the effect of training on $I \cup E$, the confidence distributions of included,
 184 excluded, and outside samples exhibit more complex overlaps: **(i)** I concentrates at high confidence,
 185 E shifts lower, while outside data often show a bimodal distribution; **(ii)** in TM-MIA, I and $E \cup O$
 186 remain partly separated but overlap substantially at high confidence; **(iii)** in SP-MIA, the distribution
 187 of $I \cup E$ largely overlaps with that of outside data, making the groups difficult to distinguish. This
 188 overlap complexity shows that model-oriented signals are no longer sufficient under subset training,
 189 highlighting the need for data-oriented alternatives.

190 4.2 CHOICE LEAKAGE ATTACK

192 **Motivation.** Just as models can overfit to their training data, subset selectors can *overfit at the selection level*: by design
 193 they preferentially reselect examples that match their implicit
 194 criteria (e.g., high informativeness, low noise, or strong repre-
 195 sentativeness). This persistent re-selection introduces a stable
 196 bias in the choice process that itself serves as a reliable mem-
 197 bership signal. We exploit this *inclusion stability*, the tendency
 198 of a sample to be repeatedly chosen across multiple trials, as
 199 the core signal for our attack.

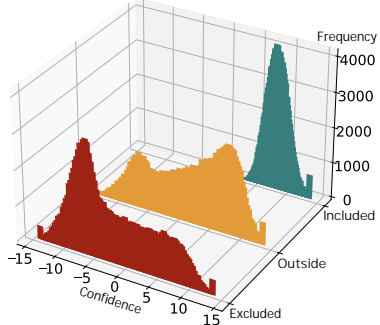
200 Specifically, we approximate many different candidate combi-
 201 nations by constructing a series of overlapping subsets (“win-
 202 dows”) $\{W_i \subseteq D_0\}_{i=1}^m$, where m is the number of windows,
 203 to capture inclusion-stable samples. Each W_i represents one
 204 plausible candidate set the selector might face; by examining
 205 the selector’s decisions on a sample across these windows, we
 206 reveal whether it is consistently favored.

207 **Subset-aware side-channel attack.** In the side-channel setting, the adversary knows both the se-
 208 lector $\text{Sel}(\cdot; r)$ and the selection ratio $r \in (0, 1]$. For each window W_i , we run $\text{Sel}(\cdot; r)$ and record
 209 whether $x \in W_i$ is selected by the selector, and get its evidence $e(x, W_i)$ in the current window:

$$e(x, W_i) = \mathbb{1}[x \in \text{Sel}(W_i; r)]. \quad (4)$$

212 Suppose in the window construction, x appears in n out of m windows; by aggregating the selection
 213 evidence across these windows, we obtain its *inclusion count*:

$$t(x) = \sum_{i=1}^n e(x, W_i), \quad (5)$$



214 Figure 2: Signal distributions of
 215 three groups of data under subset
 216 training.

216 Table 1: Results for vision models under the subset-aware side-channel attack setting. Results are
 217 averaged over 9 coresnet selection methods. *Intensity* denotes the selection ratio r (Light: $r = 0.2$,
 218 Medium: $r = 0.4$, Heavy: $r = 0.6$, Extensive: $r = 0.8$). Best results per row are in bold.
 219

220 Intensity	221 Setting	222 NN		223 NN_top3		224 NN_cls		225 LiRA		226 CoLa	
		227 AUC	228 TPR@5%FPR	229 AUC	230 TPR@5%FPR	231 AUC	232 TPR@5%FPR	233 AUC	234 TPR@5%FPR	235 AUC	236 TPR@5%FPR
227 Light	228 SP-MIA	51.23 ±2.56	229 5.83 ±1.34	230 51.77 ±3.02	231 3.34 ±4.45	232 51.59 ±2.66	233 6.37 ±2.22	234 51.26 ±4.85	235 6.43 ±3.70	236 61.39 ±2.48	237 14.24 ±2.02
	228 TM-MIA	229 64.00 ±12.15	230 12.13 ±5.96	231 61.57 ±15.05	232 8.93 ±13.52	233 67.24 ±16.18	234 19.30 ±17.14	235 69.86 ±22.08	236 15.74 ±18.19	237 83.77 ±2.44	238 42.19 ±4.51
227 Medium	228 SP-MIA	229 52.33 ±3.56	230 6.31 ±1.48	231 53.59 ±4.30	232 3.56 ±2.28	233 54.51 ±4.51	234 6.64 ±1.58	235 54.99 ±4.69	236 5.31 ±0.42	237 81.93 ±3.50	238 42.66 ±5.81
	228 TM-MIA	229 59.84 ±12.84	230 10.80 ±4.97	231 60.37 ±10.53	232 2.91 ±3.32	233 66.84 ±11.79	234 12.51 ±5.85	235 62.96 ±13.69	236 4.61 ±2.52	237 88.53 ±2.55	238 60.10 ±7.62
227 Heavy	228 SP-MIA	229 52.21 ±3.83	230 12.20 ±15.48	231 53.20 ±4.85	232 2.80 ±2.43	233 53.53 ±5.94	234 12.37 ±15.44	235 53.69 ±5.68	236 4.26 ±1.77	237 96.86 ±2.60	238 88.60 ±5.51
	228 TM-MIA	229 55.00 ±9.59	230 19.31 ±26.18	231 52.40 ±10.78	232 1.67 ±2.04	233 57.44 ±11.06	234 19.63 ±26.72	235 52.61 ±11.77	236 2.81 ±2.32	237 89.06 ±1.90	238 60.36 ±5.87
227 Extensive	228 SP-MIA	229 55.64 ±5.31	230 7.59 ±1.68	231 59.56 ±6.39	232 4.00 ±2.92	233 56.66 ±5.90	234 7.60 ±1.87	235 61.54 ±8.36	236 5.09 ±2.68	237 92.20 ±6.94	238 91.86 ±7.23
	228 TM-MIA	229 61.41 ±6.63	230 10.99 ±2.61	231 60.13 ±12.20	232 4.21 ±4.15	233 62.80 ±7.52	234 11.27 ±2.73	235 59.66 ±12.03	236 4.63 ±3.77	237 80.74 ±8.23	238 49.76 ±6.98

233 where $t(x)$ is the number of times x is selected. For fair comparison, the windows are constructed
 234 as sliding windows with fixed intervals and cyclic wrapping (details are provided in Section 5), thus
 235 each data appears in exactly the same number of windows. Hence, the exposure count n is constant
 236 across all x and serves only as a scaling factor in our score function. This also highlights the
 237 motivation behind our multi-shot membership signal: rather than relying on a single output, choice
 238 leakage signal is derived from *how consistently a sample is selected across different selections*. The
 239 membership score $s_{\text{Side}}(x)$ is obtained by aggregating evidence across windows:
 240

$$s_{\text{side}}(x, n, r) = w(t(x); n, r), \quad (6)$$

241 where w is a monotone weighting function. From a statistical perspective, if each inclusion is a
 242 Bernoulli trial, then $t(x) \sim \text{Binomial}(n(x), p(x))$ where $p(x)$ is the probability of a data to be
 243 included. Given the selection ratio r , the expected inclusion count under random choice is $r \cdot n(x)$.
 244 We can therefore design w as a smooth monotone mapping centered around $r \cdot n(x)$:

$$w(t(x); n(x), r) = \frac{\sigma(\kappa(t(x) - r \cdot n(x)))}{Z(n(x), r)}, \quad \sigma(u) = \frac{1}{1 + e^{-u}}, \quad \kappa > 0, \quad (7)$$

245 where κ controls the slope and Z is a normalization constant (depending only on $n(x), r$) that does
 246 not affect relative ranking. Since the ratio $r \in (0, 1]$ and each sample has the same exposure count
 247 n . Without loss of generality, we therefore adopt the following simplified scoring function:

$$w(t(x); n) = \sigma(t(x) - \frac{n}{2}) = \frac{1}{1 + e^{-(t(x) - \frac{n}{2})}}. \quad (8)$$

248 This formulation monotonically amplifies scores of samples with high inclusion counts and
 249 constrains the range by n , which makes scores comparable across windows. Finally, under both TM-
 250 MIA and SP-MIA, the decision is made by thresholding:

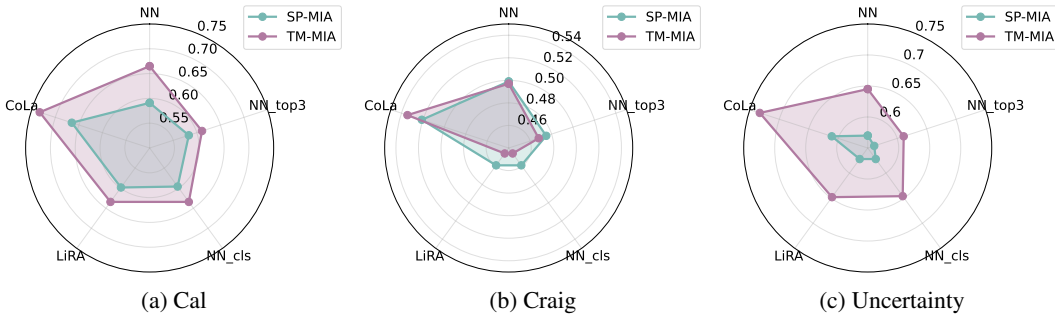
$$\hat{y}(x) = \mathbb{1}[s_{\text{side}}(x) \geq \tau], \quad (9)$$

251 where τ is a decision threshold. Samples that are more stably selected as included data across
 252 windows will receive higher scores and are thus more likely to be classified as training members.
 253

254 **Black-box attack.** In this setting, the subset selection process remains a black box to the adversary,
 255 and no direct selection metadata is available. Guided by our general motivation of *inclusion stability*
 256 (samples that are repeatedly reselected across plausible candidate sets reveal membership), we infer
 257 stable inclusion by identifying samples that consistently act as geometric representatives across
 258 windows. Specifically, for each window we perform unsupervised embedding clustering to locate
 259 representative samples. Formally, let $f(\cdot)$ be an embedding model. For each window $W_i \subseteq \mathcal{D}_i$, we
 260 compute embeddings $f(x), x \in W_i$, and perform k-means clustering (Ahmed et al., 2020) in the
 261 embedding space. Each sample $x \in W_i$ is then assigned to a cluster $c(x; W_i)$, and we measure its
 262 distance to the corresponding cluster centroid $d(x, W_i) = \|f(x) - c(x; W_i)\|_2$. The distance is used
 263 to serve as the evidence:
 264

$$e(x, W_i) = \mathbb{1}[d(x, W_i) \leq Q_{0.5}(W_i)], \quad (10)$$

270 where $Q_{0.5}(\cdot)$ is the median distance among all samples in W_i . The formal definitions of the inclusion count and exposure count follow the same formulation as in Eq. 5, with the only difference that the evidence $e(x, W_i)$ is redefined as Eq. 10 under the current black-box setting.



284 Figure 3: The MIA performance on vision models under black-box setting.

285 Here, to capture multi-shot stability, since the evidence for each data now related the distance to
 286 its centroid in each window W_i , we apply a weighted score function which reveals not only the
 287 inclusion count but also the actual distance it receives:

$$s_{\text{black}}(x) = w(t(x); n)/\bar{d}(x), \quad (11)$$

288 where $\bar{d}(x) = \frac{1}{t(x)} \sum_{i: x \in W_i} d(x, W_i)$ denotes the average clustering distance of sample x across
 289 the windows in which it is included. This design ensures that samples consistently close to cen-
 290 troids across many windows receive higher scores. The weighting function $w(t; n)$ follows the same
 291 formulation as in Eq. 8. Finally, similar to the side-channel setting, membership is determined by
 292 thresholding:

$$\hat{y}(x) = \mathbb{1}[s_{\text{black}}(x) \geq \tau]. \quad (12)$$

293 This unsupervised formulation enables membership inference even without any knowledge of the
 294 underlying subset selection metadata. The inclusion stability-based pipeline of CoLa naturally uni-
 295 fies different attack surfaces within a single framework, thereby facilitating coordinated attacks.

301 5 EXPERIMENTS

303 5.1 SETUPS

305 **Models and Datasets.** We conduct experiments on both vision and language models. For the vi-
 306 sion side, without loss of generality, we use ResNet-18 trained on CIFAR-10. We evaluate the per-
 307 formance on both subset-aware side-channel attacks and black-box attacks. For language models, since
 308 training multiple LMs from scratch is computationally expensive, we restrict our study to black-box
 309 attacks. Leveraging the rich open-source models in NLP and following the setup in (Meeus et al.,
 310 2024), we use deduplicated models from the Pythia (Biderman et al., 2023b) and GPT-Neo (Black
 311 et al., 2021) families, specifically pythia-70m, pythia-160m, and gpt-neo-125m, all trained on the
 312 MIMIR dataset (Gao et al., 2020b; Duan et al., 2024). From the MIMIR dataset, we select two sub-
 313 sets, arXiv and PubMed Central, and evaluate each under two split settings: ‘arxiv_ngram_1_0.8’,
 314 ‘arxiv_ngram_13_0.2’, ‘pubmed_central_ngram_13_0.8’, and ‘pubmed_central_ngram_13_0.2’, where
 315 ‘13_0.8’ denotes removing non-member examples that share > 80% 13-gram overlap with members.

316 In the black-box attacks for vision models, we derive embeddings from the activations just before the
 317 final linear layer of a shadow model that shares the target model’s architecture. The shadow model
 318 is trained using the GradMatch method (Killamsetty et al., 2021a) (distinct from the MIA methods
 319 evaluated in our paper) with a selection rate of 0.5. For language models, due to the various lengths
 320 of each sequence, we obtain fixed-dimensional embeddings using a dedicated embedding model; by
 321 default we use ‘all-MiniLM-L6-v2’ (Reimers & Gurevych, 2019; Thakur et al., 2021).

322 For CoLa, the default interval is set to 500 for vision models and 100 for language models, with the
 323 window size to be 20,000 and 1,000, respectively. In black-box attacks, the number of clusters is
 324 fixed at 5. Ablation studies are provided in Section 5.4.

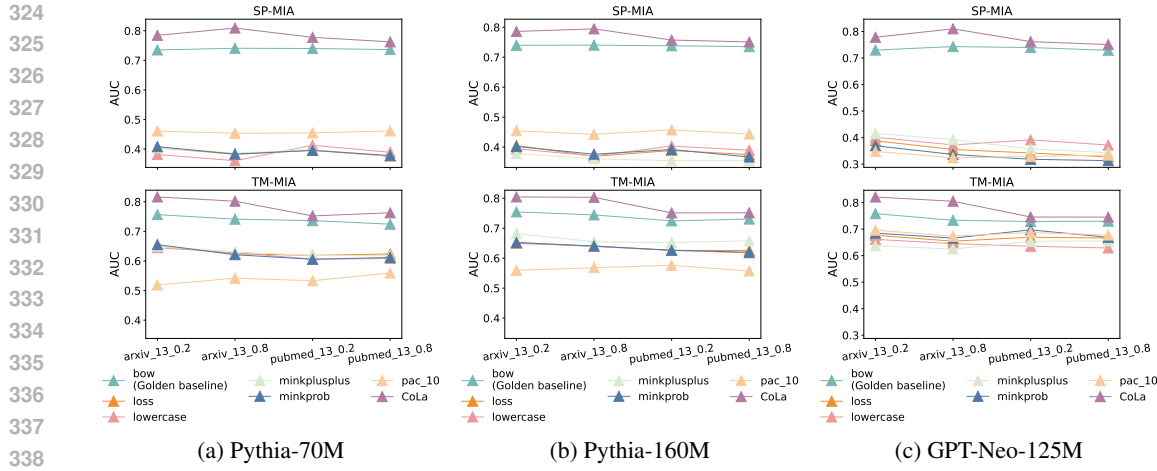


Figure 4: The MIA performance on language models under black-box setting.

Subset Selection Methods. For vision models, we select nine representative dataset pruning methods from different categories. Specifically, we include decision boundary based methods such as DeepFool (Ducoffe & Precioso, 2018) and Contrastive Active Learning (Cal) (Margatina et al., 2021); the bi-level optimization based method Glister (Killamsetty et al., 2021b); error based methods including Forgetting (Toneva et al., 2018) and GraNd (Paul et al., 2021); the uncertainty based method Least Confidence (denoted as Uncertainty) (Coleman et al., 2020); the gradient matching based method Craig (Mirzasoleiman et al., 2020); and geometry based methods such as Contextual Diversity (Agarwal et al., 2020) and Herding (Welling, 2009). These methods cover a broad range of perspectives on dataset pruning, from boundary sensitivity to optimization criteria, error contribution, uncertainty, gradient alignment, and geometric diversity. The selection ratio is set to 0.2, 0.4, 0.6, and 0.8. For language models, as discussed in the previous subsection, we adopt a commonly used data filtering strategy that has been systematically studied in (Meeus et al., 2024; Duan et al., 2024), and consider two deduplication strengths, namely ‘13_0.8’ and ‘13_0.2’.

Baseline MIA Methods. For vision models, we consider four baselines: NN, NN.top3, and NN.Cls (Shokri et al., 2017; Salem et al., 2018), which use the model’s output logits, the top-3 logits, and the combination of logits with class labels as membership signals, respectively, as well as LiRA (Carlini et al., 2022b), which fits Gaussian distributions and leverages the likelihood to infer membership. The shadow model used in each baseline method is set to 8. For language models, we consider six baselines, including the loss (Yeom et al., 2018), Lower (lowercase) (Carlini et al., 2021), Min-K% (minkprob) (Shi et al., 2023), Min-K%++ (minkplusplus) (Zhang et al., 2024), Pac (pac_10) (Ye et al., 2024), and the Golden baseline Bag_of_Words (bow) (Meeus et al., 2024). Here, bow serves as a performance reference: methods performing below it are regarded as ineffective.

Evaluation Metrics. In most MIA studies (Hisamoto et al., 2020; Carlini et al., 2022a; Li et al., 2025), attack performance is typically evaluated by aggregating over all possible thresholds using the AUC score. We adopt the same practical evaluation metric in our experiments. We also report True Positive Rate at low False Positive Rate (TPR@Low FPR) (Carlini et al., 2022b), which is an important metric in MIAs and measures the detection rate at a meaningful threshold.

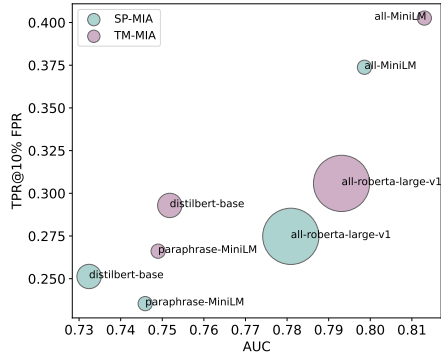
5.2 RESULTS UNDER SUBSET-AWARE SIDE-CHANNEL ATTACKS

A subset-aware side-channel attack is a type of attack specific to the subset selection process. Its success indicates that current practices of disclosing meta information about subset selection are unsafe and can lead to privacy leakage.

Table 1 reports the average MIA results across different coresnet selection methods we consider for vision models (detailed results for each method are provided in Appendix A.2). As shown, in the relatively simple TM-MIA setting, baseline methods can still perform reasonably well, which is expected since this setting closely resembles traditional MIAs (Shokri et al., 2017; Hu et al., 2022) for which these baselines were originally designed.

378 However, in the SP-MIA setting that is unique to sub-
 379 set training, baseline methods largely fail (AUC close
 380 to 50%), indicating their inability to effectively distin-
 381 guish between included and excluded data. Fundamen-
 382 tally, this stems from the fact that baseline methods rely
 383 heavily on model outputs; as illustrated in Figure 2, in-
 384 cluded and excluded data exhibit output distributions
 385 that are highly similar to other data, resulting in poor sepa-
 386 rability. However, this does not mean that privacy cannot be
 387 compromised under SP-MIA. In contrast, CoLa achieves
 388 strong performance in both TM-MIA and SP-MIA set-
 389 tings, thanks to its multi-shot, data-centric membership
 390 signal that tightly aligns with the subset selection process
 391 and captures fine-grained data interactions, thereby en-
 392 abling better separability. Moreover, we observe that as
 393 the selection ratio (*Intensity*) increases, the risk of privacy
 394 leakage becomes more severe, highlighting the significant
 395 vulnerability of the subset selection process as a potential side channel.

395 5.3 RESULTS UNDER BLACK-BOX ATTACKS



409 Figure 6: The influence of the embedding
 410 model on the MIA performance.

411 The results for vision models and language models are shown in Figure 3 and Figure 4, respectively.
 412 For vision models, we adopt three representative selection methods: Cal (Margatina et al., 2021),
 413 Craig (Mirzaoleiman et al., 2020), and Uncertainty (Coleman et al., 2020). As illustrated in Figure 3, under the black-box setting, SP-MIA remains more challenging than TM-MIA. Moreover,
 414 CoLa consistently outperforms the baselines by about 5% in AUC across all experiments, demon-
 415 strating strong attack capability. For language models, this contrast is even more pronounced. As
 416 shown in Figure 4, all baseline methods except CoLa perform worse than the bow baseline, indicat-
 417 ing that they essentially fail in the context of subset selection MIA. Furthermore, while SP-MIA and
 418 TM-MIA results are relatively close for CoLa, the baselines exhibit a sharp gap, with SP-MIA close
 419 to random guessing (AUC around 50%), and TM-MIA reaches only about 60%.

421 5.4 ABLATION STUDIES.

423 **Influence of Window Construction.** In Figure 5, we present an ablation study on the influence
 424 of window interval, conducted with Pythia-160m on the arxiv_ngram_13_0.8 dataset. Several obser-
 425 vations can be made: first, regardless of the window interval size, the performance under SP-MIA is
 426 consistently lower than that under TM-MIA, highlighting its greater challenge. Second, the choice
 427 of window interval size does not substantially affect the performance of CoLa. In SP-MIA, increas-
 428 ing the size reduces the exposure count n of each data sample, which makes the inclusion signal
 429 coarser and leads to a slight performance drop. However, this drop remains marginal.

430 **Influence of Embedding Model.** As a data-centric MIA method, CoLa achieves a clear decou-
 431 pling from the target model. As discussed earlier, it derives the membership signal by reallocat-

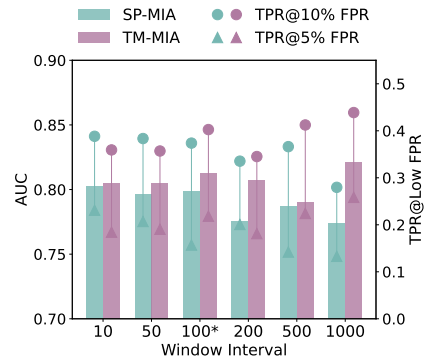


Figure 5: The influence of the window size on the MIA performance.
 leakage becomes more severe, highlighting the significant vulnerability of the subset selection process as a potential side channel.

In the black-box attack setting, we study both vision and language models. Language model subset selection often relies on heuristic semantic filtering or deduplication, rather than the formally defined selection algorithms and ratios common in vision, which makes it naturally suited to black-box analysis. In this scenario, the adversary has no access to any meta information about the selection procedure. Consequently, a successful membership inference attack under these conditions indicates that the subset selection process itself—much like model training—can implicitly reveal private information about the data. This implies that privacy risks arising from subset selection must be addressed proactively: mitigating them requires careful design choices and safeguards before the selection process is executed.

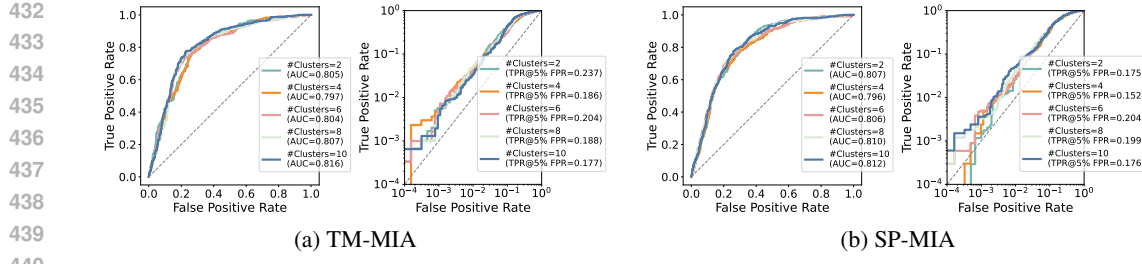


Figure 7: The MIA performance on language models under the black-box setting.

ing data combinations based on overfitting at the selection level. For language data, the inherent inconsistency in format and length requires the use of a dedicated embedding model in this reallocation process. To examine the effect of embedding model choice, we conduct an ablation study beyond the default all-MiniLM-L6-v2, considering three alternatives: paraphrase-MiniLM-L6-v2 (paraphrase-MiniLM), distilbert-base-nli-stsb-mean-tokens (distilbert-base), and all-roberta-large-v1. The results are shown in Figure 6, where the circle size indicates the parameter scale of each embedding model. We observe that different embedding models have a noticeable impact on inference performance, particularly on TPR at low FPR. Moreover, larger model size does not necessarily translate into better performance, highlighting the importance of choosing an appropriate embedding model. Nevertheless, the results remain generally acceptable across all choices (with AUC consistently above 70% and TPR@10% FPR above 25%). How to customize embedding models for MIA under subset selection is a meaningful question, which we leave for future work.

Table 2: Subset-aware Side-channel attacks under different vision models and datasets.

Setting	ResNet18-CIFAR100		VGG19-CIFAR10		VGG19-CIFAR100	
	AUC	TPR@5%FPR	AUC	TPR@5%FPR	AUC	TPR@5%FPR
SP-MIA	67.28 ±1.36	19.05 ±1.17	64.98 ±2.03	17.15 ±2.12	70.31 ±1.64	21.23 ±1.81
TM-MIA	85.53 ±2.07	38.46 ±1.43	81.43 ±1.43	40.35 ±1.65	86.67 ±2.36	42.10 ±1.39

Results under Different Vision Models and Datasets. In Table 2, we further conduct subset-aware side-channel attack on the CIFAR-100 dataset with the VGG19 model to verify whether CoLa remains reliable across different vision datasets and models. The selection ratio here is set to 0.2. As can be observed, CoLa consistently works well across various vision model–dataset combinations, revealing its general applicability. Specifically, attacks on VGG19 are more pronounced than on ResNet18 under the same setting, and CIFAR-100 is more vulnerable than CIFAR-10. Moreover, the observation that SP-MIA is more challenging than TM-MIA is consistent with previous findings.

Influence of Clustering. In Figure 7, we study the effect of varying the number of clusters used for embedding clustering in the black-box setting. Beyond the default choice of 5, we further consider values between 2 and 10 and report the corresponding AUC curves and TPR@5% FPR. The results show that, for both SP-MIA and TM-MIA, the clustering number has only a marginal effect on performance.

6 CONCLUSION

In this work, we take the first step toward systematically understanding the privacy risks of subset training. Contrary to the common intuition that training on fewer samples should reduce privacy leakage, we demonstrate that the very choices made during subset selection can themselves become exploitable signals, exposing both included and excluded data to membership inference. To capture this phenomenon, we introduced CoLa, a unified framework that leverages choice patterns to construct robust membership signals. Across both vision and language models, under both subset-aware side-channel and black-box settings, CoLa consistently outperforms existing baselines, revealing that subset training does not mitigate but instead amplifies privacy leakage. Our findings highlight that privacy risks extend beyond model outputs to the data–model supply chain itself. We hope this work motivates future efforts toward designing selection mechanisms and training pipelines that are not only efficient and scalable but also privacy-preserving.

486
487
ETHICS STATEMENT

488 This work focuses on understanding privacy risks in subset training through systematic analysis
 489 of membership inference attacks (MIAs). Our study is purely methodological and does not in-
 490 volve human subjects or personally identifiable information. All datasets used are publicly available
 491 benchmark datasets (e.g., CIFAR, GSM8K, CodeAlpaca), and we complied with their intended use
 492 and licensing terms. We emphasize that the proposed Choice Leakage Attack (CoLa) is presented
 493 as a research contribution to highlight potential vulnerabilities in modern training pipelines, not to
 494 enable misuse. Our findings are intended to inform the community about inherent privacy risks
 495 and to guide the development of stronger defenses. No proprietary or sensitive data was used, and
 496 no deployed models were targeted in this study. In line with research integrity, we also note that
 497 Large Language Models (LLMs) were only employed for literature review support and polishing of
 498 textual presentation (e.g., improving fluency and figure/table captions). LLMs were not involved in
 499 technical design, experimental implementation, or data analysis.

500
501
REPRODUCIBILITY STATEMENT

502 We have made every effort to ensure the reproducibility of our work. All datasets used in this paper
 503 are publicly available, and their sources are clearly cited in the main manuscript. The implemen-
 504 tation details of our methods, including models used, attack configurations, and evaluation protocols,
 505 are described in Section 5.1. We also provide ablation studies and additional experiments in Sec-
 506 tion 5.4 to validate the generality of our findings. Upon acceptance, we will release the full source
 507 code, configuration files, and scripts for evaluation to facilitate verification and future research.

508
509
LLM DISCLAIMER

510 LLMs were used only occasionally for language polishing, aiming to improve fluency and readabil-
 511 ity. All technical ideas, experimental designs, analyses, conclusions, writing were developed and
 512 carried out entirely by the authors. The authors have full responsibility for the final text.

535
536
REFERENCES

537 Martin Abadi, Andy Chu, Ian Goodfellow, H Brendan McMahan, Ilya Mironov, Kunal Talwar, and
 538 Li Zhang. Deep learning with differential privacy. In *Proceedings of the 2016 ACM SIGSAC
 539 conference on computer and communications security*, pp. 308–318, 2016.

540 Sharat Agarwal, Himanshu Arora, Saket Anand, and Chetan Arora. Contextual diversity for active
 541 learning. In *Computer Vision–ECCV 2020: 16th European Conference, Glasgow, UK, August
 542 23–28, 2020, Proceedings, Part XVI 16*, pp. 137–153. Springer, 2020.

543 Mohiuddin Ahmed, Raihan Seraj, and Syed Mohammed Shamsul Islam. The k-means algorithm: A
 544 comprehensive survey and performance evaluation. *Electronics*, 9(8):1295, 2020.

545 Olivier Bachem, Mario Lucic, and Andreas Krause. Coresets for nonparametric estimation—the case
 546 of dp-means. In *International Conference on Machine Learning*, pp. 209–217. PMLR, 2015.

547 Stella Biderman, Hailey Schoelkopf, Quentin Gregory Anthony, Herbie Bradley, Kyle O’Brien,
 548 Eric Hallahan, Mohammad Aflah Khan, Shivanshu Purohit, USVSN Sai Prashanth, Edward Raff,
 549 Aviya Skowron, Lintang Sutawika, and Oskar van der Wal. Pythia: A suite for analyzing large
 550 language models across training and scaling. In Andreas Krause, Emma Brunskill, Kyunghyun
 551 Cho, Barbara Engelhardt, Sivan Sabato, and Jonathan Scarlett (eds.), *International Conference
 552 on Machine Learning, ICML 2023, 23–29 July 2023, Honolulu, Hawaii, USA*, volume 202 of
 553 *Proceedings of Machine Learning Research*, pp. 2397–2430. PMLR, 2023a. URL <https://proceedings.mlr.press/v202/biderman23a.html>.

554 Stella Biderman, Hailey Schoelkopf, Quentin Gregory Anthony, Herbie Bradley, Kyle O’Brien, Eric
 555 Hallahan, Mohammad Aflah Khan, Shivanshu Purohit, USVSN Sai Prashanth, Edward Raff, et al.
 556 Pythia: A suite for analyzing large language models across training and scaling. In *International
 557 Conference on Machine Learning*, pp. 2397–2430. PMLR, 2023b.

540 Sid Black, Gao Leo, Phil Wang, Connor Leahy, and Stella Biderman. GPT-Neo: Large Scale Auto-
 541 regressive Language Modeling with Mesh-Tensorflow, March 2021. URL <https://doi.org/10.5281/zenodo.5297715>. If you use this software, please cite it using these metadata.
 542

543 Zalán Borsos, Mojmir Mutny, and Andreas Krause. Coresets via bilevel optimization for continual
 544 learning and streaming. *Advances in neural information processing systems*, 33:14879–14890,
 545 2020.

546 Nicholas Carlini, Florian Tramer, Eric Wallace, Matthew Jagielski, Ariel Herbert-Voss, Katherine
 547 Lee, Adam Roberts, Tom Brown, Dawn Song, Ulfar Erlingsson, et al. Extracting training data
 548 from large language models. In *30th USENIX security symposium (USENIX Security 21)*, pp.
 549 2633–2650, 2021.

550 Nicholas Carlini, Steve Chien, Milad Nasr, Shuang Song, Andreas Terzis, and Florian Tramèr.
 551 Membership inference attacks from first principles. In *43rd IEEE Symposium on Security and
 552 Privacy, SP 2022, San Francisco, CA, USA, May 22–26, 2022*, pp. 1897–1914. IEEE, 2022a. doi:
 553 10.1109/SP46214.2022.9833649. URL <https://doi.org/10.1109/SP46214.2022.9833649>.

554 Nicholas Carlini, Steve Chien, Milad Nasr, Shuang Song, Andreas Terzis, and Florian Tramer. Mem-
 555 bership inference attacks from first principles. In *2022 IEEE Symposium on Security and Privacy
 556 (SP)*, pp. 1897–1914. IEEE, 2022b.

557 Vincent Cohen-Addad, David Saulpic, and Chris Schwiegelshohn. A new coresnet framework for
 558 clustering. In Samir Khuller and Virginia Vassilevska Williams (eds.), *STOC '21: 53rd An-
 559 nual ACM SIGACT Symposium on Theory of Computing, Virtual Event, Italy, June 21–25, 2021*,
 560 pp. 169–182. ACM, 2021. doi: 10.1145/3406325.3451022. URL <https://doi.org/10.1145/3406325.3451022>.

561 C Coleman, C Yeh, S Mussmann, B Mirzaoleiman, P Bailis, P Liang, J Leskovec, and M Zaharia.
 562 Selection via proxy: Efficient data selection for deep learning. In *International Conference on
 563 Learning Representations (ICLR)*, 2020.

564 Tian Dong, Bo Zhao, and Lingjuan Lyu. Privacy for free: How does dataset condensation help
 565 privacy? In Kamalika Chaudhuri, Stefanie Jegelka, Le Song, Csaba Szepesvári, Gang Niu, and
 566 Sivan Sabato (eds.), *International Conference on Machine Learning, ICML 2022, 17–23 July
 567 2022, Baltimore, Maryland, USA*, volume 162 of *Proceedings of Machine Learning Research*, pp.
 568 5378–5396. PMLR, 2022. URL <https://proceedings.mlr.press/v162/dong22c.html>.

569 Michael Duan, Anshuman Suri, Niloofar Mireshghallah, Sewon Min, Weijia Shi, Luke Zettlemoyer,
 570 Yulia Tsvetkov, Yejin Choi, David Evans, and Hannaneh Hajishirzi. Do membership inference
 571 attacks work on large language models? *arXiv preprint arXiv:2402.07841*, 2024.

572 Abhimanyu Dubey, Abhinav Jauhri, Abhinav Pandey, Abhishek Kadian, Ahmad Al-Dahle, Aiesha
 573 Letman, Akhil Mathur, Alan Schelten, Amy Yang, Angela Fan, Anirudh Goyal, Anthony
 574 Hartshorn, Aobo Yang, Archi Mitra, Archie Sravankumar, Artem Korenev, Arthur Hinsvark,
 575 Arun Rao, Aston Zhang, Aurélien Rodriguez, Austen Gregerson, Ava Spataru, Baptiste Rozière,
 576 Bethany Biron, Binh Tang, Bobbie Chern, Charlotte Caucheteux, Chaya Nayak, Chloe Bi, Chris
 577 Marra, Chris McConnell, Christian Keller, Christophe Touret, Chunyang Wu, Corinne Wong,
 578 Cristian Canton Ferrer, Cyrus Nikolaidis, Damien Allonsius, Daniel Song, Danielle Pintz, Danny
 579 Livshits, David Esiobu, Dhruv Choudhary, Dhruv Mahajan, Diego Garcia-Olano, Diego Perino,
 580 Dieuwke Hupkes, Egor Lakomkin, Ehab AlBadawy, Elina Lobanova, Emily Dinan, Eric Michael
 581 Smith, Filip Radenovic, Frank Zhang, Gabriel Synnaeve, Gabrielle Lee, Georgia Lewis Ander-
 582 son, Graeme Nail, Grégoire Mialon, Guan Pang, Guillem Cucurell, Hailey Nguyen, Hannah Ko-
 583 revaar, Hu Xu, Hugo Touvron, Iliyan Zarov, Imanol Arrieta Ibarra, Isabel M. Kloumann, Ishan
 584 Misra, Ivan Evtimov, Jade Copet, Jaewon Lee, Jan Geffert, Jana Vrana, Jason Park, Jay Ma-
 585 hadeokar, Jeet Shah, Jelmer van der Linde, Jennifer Billock, Jenny Hong, Jenya Lee, Jeremy
 586 Fu, Jianfeng Chi, Jianyu Huang, Jiawen Liu, Jie Wang, Jiecao Yu, Joanna Bitton, Joe Spisak,
 587 Jongsoo Park, Joseph Rocca, Joshua Johnstun, Joshua Saxe, Junteng Jia, Kalyan Vasudeni Al-
 588 wala, Kartikeya Upasani, Kate Plawiak, Ke Li, Kenneth Heafield, Kevin Stone, and et al. The

594 llama 3 herd of models. *CoRR*, abs/2407.21783, 2024. doi: 10.48550/ARXIV.2407.21783. URL
 595 <https://doi.org/10.48550/arXiv.2407.21783>.
 596

597 Melanie Ducoffe and Frederic Precioso. Adversarial active learning for deep networks: a margin
 598 based approach. *arXiv preprint arXiv:1802.09841*, 2018.

599 Leo Gao, Stella Biderman, Sid Black, Laurence Golding, Travis Hoppe, Charles Foster, Jason
 600 Phang, Horace He, Anish Thite, Noa Nabeshima, Shawn Presser, and Connor Leahy. The pile:
 601 An 800gb dataset of diverse text for language modeling, 2020a. URL <https://arxiv.org/abs/2101.00027>.
 602

603 Leo Gao, Stella Biderman, Sid Black, Laurence Golding, Travis Hoppe, Charles Foster, Jason
 604 Phang, Horace He, Anish Thite, Noa Nabeshima, et al. The pile: An 800gb dataset of diverse text
 605 for language modeling. *arXiv preprint arXiv:2101.00027*, 2020b.

606 Suriya Gunasekar, Yi Zhang, Jyoti Aneja, Caio César Teodoro Mendes, Allie Del Giorno, Sivakanth
 607 Gopi, Mojan Javaheripi, Piero Kauffmann, Gustavo de Rosa, Olli Saarikivi, Adil Salim, Shital
 608 Shah, Harkirat Singh Behl, Xin Wang, Sébastien Bubeck, Ronen Eldan, Adam Tauman Kalai,
 609 Yin Tat Lee, and Yuanzhi Li. Textbooks are all you need. *CoRR*, abs/2306.11644, 2023. doi: 10.
 610 48550/ARXIV.2306.11644. URL <https://doi.org/10.48550/arXiv.2306.11644>.
 611

612 Sorami Hisamoto, Matt Post, and Kevin Duh. Membership inference attacks on sequence-to-
 613 sequence models: Is my data in your machine translation system? *Transactions of the As-
 614 sociation for Computational Linguistics*, 8:49–63, 2020. doi: 10.1162/tacl_a_00299. URL
 615 <https://aclanthology.org/2020.tacl-1.4/>.

616 Hongsheng Hu, Zoran Salcic, Lichao Sun, Gillian Dobbie, Philip S Yu, and Xuyun Zhang. Mem-
 617 bership inference attacks on machine learning: A survey. *ACM Computing Surveys (CSUR)*, 54
 618 (11s):1–37, 2022.

619 Yuzheng Hu, Fan Wu, Qinbin Li, Yunhui Long, Gonzalo Munilla Garrido, Chang Ge, Bolin Ding,
 620 David Forsyth, Bo Li, and Dawn Song. Sok: Privacy-preserving data synthesis. In *2024 IEEE
 621 Symposium on Security and Privacy (SP)*, pp. 4696–4713, 2024. doi: 10.1109/SP54263.2024.
 622 00002.

623 Krishnateja Killamsetty, Sivasubramanian Durga, Ganesh Ramakrishnan, Abir De, and Rishabh
 624 Iyer. Grad-match: Gradient matching based data subset selection for efficient deep model training.
 625 In *International Conference on Machine Learning*, pp. 5464–5474. PMLR, 2021a.

626 Krishnateja Killamsetty, Durga Sivasubramanian, Ganesh Ramakrishnan, and Rishabh Iyer. Glister:
 627 Generalization based data subset selection for efficient and robust learning. In *Proceedings of the
 628 AAAI Conference on Artificial Intelligence*, volume 35, pp. 8110–8118, 2021b.

629 Katherine Lee, Daphne Ippolito, Andrew Nystrom, Chiyuan Zhang, Douglas Eck, Chris Callison-
 630 Burch, and Nicholas Carlini. Deduplicating training data makes language models better. In
 631 Smaranda Muresan, Preslav Nakov, and Aline Villavicencio (eds.), *Proceedings of the 60th An-
 632 nual Meeting of the Association for Computational Linguistics (Volume 1: Long Papers)*, pp.
 633 8424–8445, Dublin, Ireland, May 2022. Association for Computational Linguistics. doi: 10.
 634 18653/v1/2022.acl-long.577. URL <https://aclanthology.org/2022.acl-long.577/>.

635 Qi Li, Runpeng Yu, and Xinchao Wang. Vid-sme: Membership inference attacks against large video
 636 understanding models. *arXiv preprint arXiv:2506.03179*, 2025.

637 Adyasha Maharana, Prateek Yadav, and Mohit Bansal. D2 pruning: Message passing for balanc-
 638 ing diversity & difficulty in data pruning. In *The Twelfth International Conference on Learning
 639 Representations*, 2023.

640 Katerina Margatina, Giorgos Vernikos, Loïc Barrault, and Nikolaos Aletras. Active learning by
 641 acquiring contrastive examples. pp. 650–663, 2021. doi: 10.18653/V1/2021.EMNLP-MAIN.51.
 642 URL <https://doi.org/10.18653/v1/2021.emnlp-main.51>.

648 Matthieu Meeus, Igor Shilov, Shubham Jain, Manuel Faysse, Marek Rei, and Yves-Alexandre
 649 de Montjoye. Sok: Membership inference attacks on llms are rushing nowhere (and how to
 650 fix it). *arXiv preprint arXiv:2406.17975*, 2024.

651 Baharan Mirzasoleiman, Jeff Bilmes, and Jure Leskovec. Coresets for data-efficient training of
 652 machine learning models. In *International Conference on Machine Learning*, pp. 6950–6960.
 653 PMLR, 2020.

654 Alexander Munteanu, Chris Schwiegelshohn, Christian Sohler, and David Woodruff. On coresets
 655 for logistic regression. *Advances in Neural Information Processing Systems*, 31, 2018.

656 Milad Nasr, Reza Shokri, and Amir Houmansadr. Machine learning with membership privacy using
 657 adversarial regularization. In *Proceedings of the 2018 ACM SIGSAC Conference on Computer and
 658 Communications Security*, CCS ’18, pp. 634–646, New York, NY, USA, 2018. Association for
 659 Computing Machinery. ISBN 9781450356930. doi: 10.1145/3243734.3243855. URL <https://doi.org/10.1145/3243734.3243855>.

660 Mansheej Paul, Surya Ganguli, and Gintare Karolina Dziugaite. Deep learning on a data diet: Find-
 661 ing important examples early in training. *Advances in Neural Information Processing Systems*,
 662 34:20596–20607, 2021.

663 Ru Peng, Kexin Yang, Yawen Zeng, Junyang Lin, Dayiheng Liu, and Junbo Zhao. Dataman:
 664 Data manager for pre-training large language models. In *The Thirteenth International Confer-
 665 ence on Learning Representations*, 2025. URL <https://openreview.net/forum?id=eNbA8Fqir4>.

666 Ziheng Qin, Kai Wang, Zangwei Zheng, Jianyang Gu, Xiangyu Peng, Daquan Zhou, Lei Shang,
 667 Baigui Sun, Xuansong Xie, Yang You, et al. Infobatch: Lossless training speed up by unbiased
 668 dynamic data pruning. In *The Twelfth International Conference on Learning Representations*,
 669 2023.

670 Jack W. Rae, Sebastian Borgeaud, Trevor Cai, Katie Millican, Jordan Hoffmann, H. Francis
 671 Song, John Aslanides, Sarah Henderson, Roman Ring, Susannah Young, Eliza Rutherford,
 672 Tom Hennigan, Jacob Menick, Albin Cassirer, Richard Powell, George van den Driessche,
 673 Lisa Anne Hendricks, Maribeth Rauh, Po-Sen Huang, Amelia Glaese, Johannes Welbl, Sumanth
 674 Dathathri, Saffron Huang, Jonathan Uesato, John Mellor, Irina Higgins, Antonia Creswell, Nat
 675 McAleese, Amy Wu, Erich Elsen, Siddhant M. Jayakumar, Elena Buchatskaya, David Budden,
 676 Esme Sutherland, Karen Simonyan, Michela Paganini, Laurent Sifre, Lena Martens, Xiang Lor-
 677 raine Li, Adhiguna Kuncoro, Aida Nematzadeh, Elena Gribovskaya, Domenic Donato, Ange-
 678 liki Lazaridou, Arthur Mensch, Jean-Baptiste Lespiau, Maria Tsimpoukelli, Nikolai Grigorev,
 679 Doug Fritz, Thibault Sotiaux, Mantas Pajarskas, Toby Pohlen, Zhitao Gong, Daniel Toyama, Cy-
 680 prien de Masson d’Autume, Yujia Li, Tayfun Terzi, Vladimir Mikulik, Igor Babuschkin, Aidan
 681 Clark, Diego de Las Casas, Aurelia Guy, Chris Jones, James Bradbury, Matthew J. Johnson,
 682 Blake A. Hechtman, Laura Weidinger, Iason Gabriel, William Isaac, Edward Lockhart, Simon
 683 Osindero, Laura Rimell, Chris Dyer, Oriol Vinyals, Kareem Ayoub, Jeff Stanway, Lorrayne
 684 Bennett, Demis Hassabis, Koray Kavukcuoglu, and Geoffrey Irving. Scaling language mod-
 685 els: Methods, analysis & insights from training gopher. *CoRR*, abs/2112.11446, 2021. URL
 686 <https://arxiv.org/abs/2112.11446>.

687 Colin Raffel, Noam Shazeer, Adam Roberts, Katherine Lee, Sharan Narang, Michael Matena, Yanqi
 688 Zhou, Wei Li, and Peter J. Liu. Exploring the limits of transfer learning with a unified text-to-text
 689 transformer, 2023. URL <https://arxiv.org/abs/1910.10683>.

690 Nils Reimers and Iryna Gurevych. Sentence-bert: Sentence embeddings using siamese bert-
 691 networks. In *Proceedings of the 2019 Conference on Empirical Methods in Natural Language
 692 Processing*. Association for Computational Linguistics, 11 2019. URL <https://arxiv.org/abs/1908.10084>.

693 Alexandre Sablayrolles, Matthijs Douze, Cordelia Schmid, Yann Ollivier, and Hervé Jégou. White-
 694 box vs black-box: Bayes optimal strategies for membership inference. In Kamalika Chaudhuri
 695 and Ruslan Salakhutdinov (eds.), *Proceedings of the 36th International Conference on Machine
 696 Learning, ICML 2019, 9-15 June 2019, Long Beach, California, USA*, volume 97 of *Proceedings
 697 of Machine Learning*, 2019. URL <https://proceedings.mlr.press/v97/sablayrolles19a.html>.

698

702 *of Machine Learning Research*, pp. 5558–5567. PMLR, 2019. URL <http://proceedings.mlr.press/v97/sablayrolles19a.html>.

703

704

705 Ahmed Salem, Yang Zhang, Mathias Humbert, Pascal Berrang, Mario Fritz, and Michael Backes.
 706 MI-leaks: Model and data independent membership inference attacks and defenses on machine
 707 learning models. *arXiv preprint arXiv:1806.01246*, 2018.

708

709 Ozan Sener and Silvio Savarese. Active learning for convolutional neural networks: A core-set
 710 approach. 2018. URL <https://openreview.net/forum?id=H1aIuk-RW>.

711

712 Weijia Shi, Anirudh Ajith, Mengzhou Xia, Yangsibo Huang, Daogao Liu, Terra Blevins, Danqi
 713 Chen, and Luke Zettlemoyer. Detecting pretraining data from large language models. *arXiv
 714 preprint arXiv:2310.16789*, 2023.

715

716 Reza Shokri, Marco Stronati, Congzheng Song, and Vitaly Shmatikov. Membership inference at-
 717 tacks against machine learning models. In *2017 IEEE symposium on security and privacy (SP)*,
 718 pp. 3–18. IEEE, 2017.

719

720 Ben Sorscher, Robert Geirhos, Shashank Shekhar, Surya Ganguli, and Ari Morcos. Beyond neu-
 721 ral scaling laws: beating power law scaling via data pruning. *Advances in Neural Information
 722 Processing Systems*, 35:19523–19536, 2022.

723

724 Theresa Stadler, Bristena Oprisanu, and Carmela Troncoso. Synthetic data - anonymisation ground-
 725 hog day. In Kevin R. B. Butler and Kurt Thomas (eds.), *31st USENIX Security Symposium,
 726 USENIX Security 2022, Boston, MA, USA, August 10-12, 2022*, pp. 1451–1468. USENIX Asso-
 727 ciation, 2022. URL <https://www.usenix.org/conference/usenixsecurity22/presentation/stadler>.

728

729 Bowen Tan, Zheng Xu, Eric P. Xing, Zhiting Hu, and Shanshan Wu. Synthesizing privacy-preserving
 730 text data via finetuning *without* finetuning billion-scale LLMs. In *Forty-second International
 731 Conference on Machine Learning*, 2025. URL <https://openreview.net/forum?id=FCm4laCLiH>.

732

733 Haoru Tan, Sitong Wu, Fei Du, Yukang Chen, Zhibin Wang, Fan Wang, and Xiaojuan Qi. Data
 734 pruning via moving-one-sample-out. *Advances in Neural Information Processing Systems*, 36,
 735 2024.

736

737 Nandan Thakur, Nils Reimers, Johannes Daxenberger, and Iryna Gurevych. Augmented SBERT:
 738 Data augmentation method for improving bi-encoders for pairwise sentence scoring tasks. In
 739 *Proceedings of the 2021 Conference of the North American Chapter of the Association for Com-
 740 putational Linguistics: Human Language Technologies*, pp. 296–310, Online, June 2021. As-
 741 sociation for Computational Linguistics. URL <https://www.aclweb.org/anthology/2021.naacl-main.28>.

742

743 Mariya Toneva, Alessandro Sordoni, Remi Tachet des Combes, Adam Trischler, Yoshua Bengio,
 744 and Geoffrey J Gordon. An empirical study of example forgetting during deep neural network
 745 learning. In *International Conference on Learning Representations*, 2018.

746

747 Boris van Breugel, Hao Sun, Zhaozhi Qian, and Mihaela van der Schaar. Membership inference
 748 attacks against synthetic data through overfitting detection. In Francisco J. R. Ruiz, Jennifer G.
 749 Dy, and Jan-Willem van de Meent (eds.), *International Conference on Artificial Intelligence and
 750 Statistics, 25-27 April 2023, Palau de Congressos, Valencia, Spain*, volume 206 of *Proceedings of
 751 Machine Learning Research*, pp. 3493–3514. PMLR, 2023. URL <https://proceedings.mlr.press/v206/breugel23a.html>.

752

753 Max Welling. Herding dynamical weights to learn. In *Proceedings of the 26th annual international
 754 conference on machine learning*, pp. 1121–1128, 2009.

755

756 Alexander Wettig, Aatmik Gupta, Saumya Malik, and Danqi Chen. Qurating: selecting high-quality
 757 data for training language models. In *Proceedings of the 41st International Conference on Ma-
 758 chine Learning*, ICML’24. JMLR.org, 2024.

756 An Yang, Baosong Yang, Beichen Zhang, Binyuan Hui, Bo Zheng, Bowen Yu, Chengyuan Li,
 757 Dayiheng Liu, Fei Huang, Haoran Wei, Huan Lin, Jian Yang, Jianhong Tu, Jianwei Zhang, Jianxin
 758 Yang, Jiaxi Yang, Jingren Zhou, Junyang Lin, Kai Dang, Keming Lu, Keqin Bao, Kexin Yang,
 759 Le Yu, Mei Li, Mingfeng Xue, Pei Zhang, Qin Zhu, Rui Men, Runji Lin, Tianhao Li, Tingyu
 760 Xia, Xingzhang Ren, Xuancheng Ren, Yang Fan, Yang Su, Yichang Zhang, Yu Wan, Yuqiong
 761 Liu, Zeyu Cui, Zhenru Zhang, and Zihan Qiu. Qwen2.5 technical report. *CoRR*, abs/2412.15115,
 762 2024a. doi: 10.48550/ARXIV.2412.15115. URL <https://doi.org/10.48550/arXiv.2412.15115>.

763

764 Shuo Yang, Zeke Xie, Hanyu Peng, Min Xu, Mingming Sun, and Ping Li. Dataset pruning: Reduc-
 765 ing training data by examining generalization influence. In *The Eleventh International Conference
 766 on Learning Representations*, 2022.

767

768 Shuo Yang, Zhe Cao, Sheng Guo, Ruiheng Zhang, Ping Luo, Shengping Zhang, and Liqiang Nie.
 769 Mind the boundary: Coreset selection via reconstructing the decision boundary. In *Forty-first
 770 International Conference on Machine Learning*, 2024b.

771 Wentao Ye, Jiaqi Hu, Liyao Li, Haobo Wang, Gang Chen, and Junbo Zhao. Data contamination
 772 calibration for black-box llms. *arXiv preprint arXiv:2405.11930*, 2024.

773

774 Samuel Yeom, Irene Giacomelli, Matt Fredrikson, and Somesh Jha. Privacy risk in machine learn-
 775 ing: Analyzing the connection to overfitting. In *2018 IEEE 31st computer security foundations
 776 symposium (CSF)*, pp. 268–282. IEEE, 2018.

777 Jingyang Zhang, Jingwei Sun, Eric Yeats, Yang Ouyang, Martin Kuo, Jianyi Zhang, Hao Frank
 778 Yang, and Hai Li. Min-k%++: Improved baseline for detecting pre-training data from large
 779 language models. *arXiv preprint arXiv:2404.02936*, 2024.

780 Yunpeng Zhao and Jie Zhang. Does training with synthetic data truly protect privacy? In
 781 *The Thirteenth International Conference on Learning Representations*, 2025. URL <https://openreview.net/forum?id=C8niXBHjfO>.

782

783

784

785

786

787

788

789

790

791

792

793

794

795

796

797

798

799

800

801

802

803

804

805

806

807

808

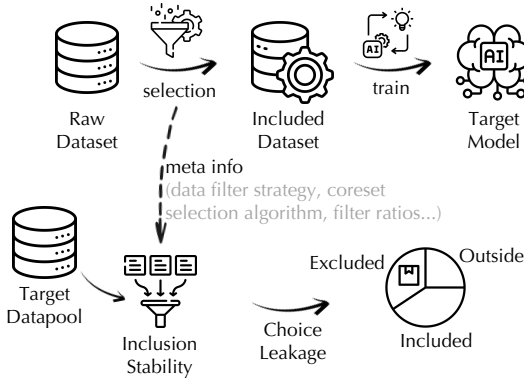
809

810
811
812
813
814
815
816
817
818
819
820
821
822
823
824
825
826

A APPENDIX

827
828
829
830
831
832
833
834

A.1 THE PRIVACY THREATS BEHIND DATA-MODEL SUPPLY CHAIN



827
828
829
830
831
832
833
834
Figure 8: Choice Leakage Attack (CoLa) across the data–model supply chain. CoLa augments conventional MIA by exploiting subset selection metadata leaked along the data–model supply chain. By identifying which samples are more likely to pass selection, it not only strengthens membership inference but also enables adversaries to craft tailored threats.

835
836
837
838
839
choice leakage risk is severe as it not only amplifies the risk of inferring membership but also exposes a system’s selection preferences. Once the data–model supply chain is exposed to privacy risks, the entire pipeline, from raw data to model outputs, becomes vulnerable to malicious manipulation. For example, adversaries may learn proxies of the selection rule and craft targeted poisoning or backdoor examples that are more likely to bypass filtering and enter training.

840
841
842
Table 3: The results of vision models under Subset-aware Side-channel attacks and the subset selec-
843
844
845
846
847
848
849
850
851
852
853
854
855
856
857
858
859
860
861
862
863
tion method used here is Cal (Margatina et al., 2021).

Intensity	Setting	NN		NN_top3		NN_cls		LiRA		CoLa	
		AUC	TPR@5%FPR	AUC	TPR@5%FPR	AUC	TPR@5%FPR	AUC	TPR@5%FPR	AUC	TPR@5%FPR
Light	SP-MIA	0.499	0.050	0.501	0.055	0.508	0.053	0.512	0.054	0.602	0.122
	TM-MIA	0.759	0.207	0.676	0.166	0.784	0.257	0.737	0.182	0.855	0.442
Medium	SP-MIA	0.553	0.072	0.573	0.056	0.582	0.074	0.587	0.058	0.789	0.372
	TM-MIA	0.763	0.165	0.759	0.097	0.812	0.227	0.784	0.092	0.878	0.620
Heavy	SP-MIA	0.589	0.077	0.603	0.000	0.630	0.087	0.624	0.054	0.963	0.856
	TM-MIA	0.729	0.123	0.721	0.000	0.772	0.172	0.736	0.058	0.895	0.642
Extensive	SP-MIA	0.634	0.091	0.637	0.000	0.647	0.092	0.651	0.036	0.957	0.954
	TM-MIA	0.717	0.116	0.707	0.061	0.736	0.128	0.690	0.026	0.849	0.573

853
854
855
Table 4: The results of vision models under Subset-aware Side-channel attacks and the subset selec-
856
857
858
859
860
861
862
863
tion method used here is Contextual Diverstiy (Agarwal et al., 2020).

Intensity	Setting	NN		NN_top3		NN_cls		LiRA		CoLa	
		AUC	TPR@5%FPR	AUC	TPR@5%FPR	AUC	TPR@5%FPR	AUC	TPR@5%FPR	AUC	TPR@5%FPR
Light	SP-MIA	0.540	0.067	0.539	0.053	0.548	0.073	0.544	0.052	0.633	0.118
	TM-MIA	0.706	0.125	0.716	0.070	0.755	0.161	0.756	0.072	0.798	0.347
Medium	SP-MIA	0.598	0.094	0.594	0.000	0.614	0.088	0.610	0.056	0.846	0.465
	TM-MIA	0.751	0.158	0.708	0.000	0.792	0.160	0.729	0.049	0.908	0.656
Heavy	SP-MIA	0.507	0.051	0.502	0.000	0.506	0.500	0.500	0.000	0.982	0.904
	TM-MIA	0.502	0.074	0.482	0.000	0.516	0.048	0.477	0.000	0.898	0.631
Extensive	SP-MIA	0.494	0.056	0.494	0.027	0.497	0.052	0.497	0.042	0.967	0.966
	TM-MIA	0.500	0.053	0.490	0.000	0.502	0.052	0.490	0.041	0.843	0.386

864 A.2 RESULTS OF VISION MODELS UNDER DIFFERENT SUBSET SELECTION METHODS
865866 In Table 1, we report the average results of vision models across nine subset selection methods. For
867 clarity, Tables 3–11 present the results for each method separately, providing a more straightforward
868 view of the attack performance.869 Table 5: The results of vision models under Subset-aware Side-channel attacks and the subset selec-
870 tion method used here is Craig (Mirzasoleiman et al., 2020).
871

Intensity	Setting	NN		NN_top3		NN_cls		LiRA		CoLa	
		AUC	TPR@5%FPR	AUC	TPR@5%FPR	AUC	TPR@5%FPR	AUC	TPR@5%FPR	AUC	TPR@5%FPR
Light	SP-MIA	0.495	0.046	0.500	0.000	0.497	0.048	0.441	0.039	0.637	0.172
	TM-MIA	0.567	0.087	0.500	0.000	0.573	0.102	0.602	0.064	0.825	0.411
Medium	SP-MIA	0.513	0.066	0.588	0.054	0.580	0.086	0.598	0.055	0.819	0.367
	TM-MIA	0.595	0.137	0.693	0.043	0.717	0.134	0.716	0.045	0.858	0.518
Heavy	SP-MIA	0.575	0.076	0.614	0.052	0.628	0.082	0.629	0.051	0.969	0.876
	TM-MIA	0.624	0.114	0.628	0.030	0.701	0.122	0.647	0.034	0.888	0.562
Extensive	SP-MIA	0.624	0.092	0.655	0.000	0.653	0.096	0.664	0.000	0.960	0.959
	TM-MIA	0.674	0.110	0.666	0.000	0.700	0.119	0.623	0.000	0.842	0.545

880
881 Table 6: The results of vision models under Subset-aware Side-channel attacks and the subset selec-
882 tion method used here is DeepFool (Ducoffe & Precioso, 2018).
883

Intensity	Setting	NN		NN_top3		NN_cls		LiRA		CoLa	
		AUC	TPR@5%FPR	AUC	TPR@5%FPR	AUC	TPR@5%FPR	AUC	TPR@5%FPR	AUC	TPR@5%FPR
Light	SP-MIA	0.494	0.057	0.500	0.000	0.489	0.054	0.441	0.039	0.637	0.172
	TM-MIA	0.556	0.092	0.500	0.000	0.530	0.084	0.221	0.000	0.825	0.411
Medium	SP-MIA	0.494	0.051	0.501	0.048	0.492	0.050	0.500	0.050	0.845	0.480
	TM-MIA	0.649	0.088	0.550	0.000	0.642	0.088	0.397	0.011	0.926	0.700
Heavy	SP-MIA	0.496	0.053	0.507	0.000	0.496	0.052	0.509	0.042	0.979	0.900
	TM-MIA	0.494	0.053	0.429	0.016	0.484	0.054	0.424	0.000	0.902	0.643
Extensive	SP-MIA	0.526	0.096	0.643	0.062	0.545	0.097	0.645	0.067	0.956	0.954
	TM-MIA	0.592	0.142	0.571	0.037	0.602	0.140	0.574	0.038	0.858	0.572

892
893 Table 7: The results of vision models under Subset-aware Side-channel attacks and the subset selec-
894 tion method used here is Forgetting (Toneva et al., 2018).
895

Intensity	Setting	NN		NN_top3		NN_cls		LiRA		CoLa	
		AUC	TPR@5%FPR	AUC	TPR@5%FPR	AUC	TPR@5%FPR	AUC	TPR@5%FPR	AUC	TPR@5%FPR
Light	SP-MIA	0.500	0.053	0.500	0.000	0.514	0.059	0.530	0.051	0.618	0.141
	TM-MIA	0.572	0.099	0.500	0.000	0.706	0.176	0.741	0.071	0.854	0.475
Medium	SP-MIA	0.503	0.056	0.500	0.000	0.548	0.068	0.559	0.056	0.818	0.464
	TM-MIA	0.529	0.098	0.500	0.000	0.695	0.139	0.724	0.064	0.851	0.517
Heavy	SP-MIA	0.501	0.500	0.499	0.045	0.499	0.050	0.498	0.050	0.986	0.943
	TM-MIA	0.540	0.830	0.480	0.000	0.546	0.840	0.460	0.034	0.921	0.661
Extensive	SP-MIA	0.585	0.080	0.640	0.071	0.585	0.081	0.748	0.084	0.791	0.787
	TM-MIA	0.646	0.107	0.640	0.074	0.649	0.107	0.648	0.080	0.653	0.407

903
904
905
906
907
908
909
910
911
912
913
914
915
916
917

918

919

920 Table 8: The results of vision models under Subset-aware Side-channel attacks and the subset selec-
921 tion method used here is Glister (Killamsetty et al., 2021b).

Intensity	Setting	NN		NN_top3		NN_cls		LiRA		CoLa	
		AUC	TPR@5%FPR	AUC	TPR@5%FPR	AUC	TPR@5%FPR	AUC	TPR@5%FPR	AUC	TPR@5%FPR
Light	SP-MIA	0.495	0.048	0.500	0.000	0.492	0.045	0.545	0.062	0.608	0.135
	TM-MIA	0.477	0.033	0.500	0.000	0.422	0.000	0.883	0.129	0.829	0.384
Medium	SP-MIA	0.504	0.055	0.497	0.044	0.503	0.049	0.496	0.045	0.864	0.494
	TM-MIA	0.367	0.007	0.545	0.045	0.448	0.024	0.586	0.044	0.874	0.516
Heavy	SP-MIA	0.494	0.050	0.499	0.048	0.495	0.048	0.497	0.051	0.992	0.949
	TM-MIA	0.404	0.039	0.541	0.060	0.440	0.020	0.555	0.059	0.871	0.480
Extensive	SP-MIA	0.527	0.062	0.598	0.073	0.533	0.060	0.600	0.079	0.984	0.984
	TM-MIA	0.598	0.131	0.757	0.118	0.651	0.134	0.771	0.120	0.895	0.502

930

931

932

933 Table 9: The results of vision models under Subset-aware Side-channel attacks and the subset selec-
934 tion method used here is GraNd (Paul et al., 2021).

Intensity	Setting	NN		NN_top3		NN_cls		LiRA		CoLa	
		AUC	TPR@5%FPR	AUC	TPR@5%FPR	AUC	TPR@5%FPR	AUC	TPR@5%FPR	AUC	TPR@5%FPR
Light	SP-MIA	0.563	0.087	0.584	0.126	0.563	0.114	0.575	0.153	0.562	0.137
	TM-MIA	0.843	0.206	0.918	0.389	0.937	0.571	0.950	0.584	0.878	0.483
Medium	SP-MIA	0.498	0.048	0.498	0.047	0.497	0.050	0.499	0.052	0.754	0.344
	TM-MIA	0.535	0.103	0.471	0.019	0.573	0.104	0.471	0.018	0.902	0.680
Heavy	SP-MIA	0.493	0.047	0.500	0.051	0.493	0.047	0.501	0.050	0.909	0.774
	TM-MIA	0.557	0.119	0.387	0.011	0.562	0.118	0.384	0.012	0.859	0.606
Extensive	SP-MIA	0.505	0.054	0.502	0.047	0.506	0.054	0.503	0.048	0.839	0.826
	TM-MIA	0.572	0.110	0.378	0.005	0.556	0.109	0.380	0.019	0.712	0.498

944

945

946

947 Table 10: The results of vision models under Subset-aware Side-channel attacks and the subset
948 selection method used here is Herding (Welling, 2009).

Intensity	Setting	NN		NN_top3		NN_cls		LiRA		CoLa	
		AUC	TPR@5%FPR	AUC	TPR@5%FPR	AUC	TPR@5%FPR	AUC	TPR@5%FPR	AUC	TPR@5%FPR
Light	SP-MIA	0.516	0.053	0.521	0.052	0.512	0.054	0.510	0.053	0.574	0.171
	TM-MIA	0.853	0.407	0.912	0.373	0.932	0.452	0.927	0.389	0.963	0.771
Medium	SP-MIA	0.498	0.050	0.498	0.051	0.498	0.049	0.499	0.051	0.753	0.460
	TM-MIA	0.857	0.244	0.749	0.092	0.861	0.246	0.757	0.088	0.976	0.880
Heavy	SP-MIA	0.543	0.061	0.601	0.059	0.545	0.078	0.600	0.067	0.966	0.846
	TM-MIA	0.782	0.210	0.740	0.029	0.792	0.206	0.741	0.028	0.931	0.729
Extensive	SP-MIA	0.491	0.047	0.498	0.000	0.492	0.049	0.497	0.043	0.964	0.963
	TM-MIA	0.687	0.127	0.542	0.046	0.688	0.126	0.542	0.049	0.862	0.571

957

958

959

960

961 Table 11: The results of vision models under Subset-aware Side-channel attacks and the subset
962 selection method used here is Uncertainty (Coleman et al., 2020).

Intensity	Setting	NN		NN_top3		NN_cls		LiRA		CoLa	
		AUC	TPR@5%FPR	AUC	TPR@5%FPR	AUC	TPR@5%FPR	AUC	TPR@5%FPR	AUC	TPR@5%FPR
Light	SP-MIA	0.499	0.051	0.499	0.054	0.499	0.049	0.498	0.050	0.603	0.138
	TM-MIA	0.549	0.065	0.458	0.021	0.528	0.063	0.437	0.019	0.827	0.376
Medium	SP-MIA	0.494	0.050	0.498	0.050	0.494	0.05	0.496	0.050	0.811	0.454
	TM-MIA	0.614	0.073	0.444	0.020	0.610	0.072	0.433	0.019	0.914	0.703
Heavy	SP-MIA	0.554	0.089	0.625	0.054	0.560	0.089	0.627	0.051	0.959	0.850
	TM-MIA	0.709	0.13	0.644	0.025	0.713	0.130	0.644	0.025	0.899	0.644
Extensive	SP-MIA	0.501	0.050	0.506	0.044	0.502	0.051	0.502	0.050	0.929	0.924
	TM-MIA	0.614	0.117	0.424	0.000	0.607	0.118	0.425	0.03	0.823	0.575

971